The Effect of Nano-Sized Silicate Layers from Montmorillonite on Glass Transition, Dynamic Mechanical, and Thermal Degradation Properties of Segmented Polyurethane

Yun. I. Tien, Kung Hwa Wei

Department of Materials Science and Engineering, National Chiao Tung University, Hsinchu, Taiwan 30049, Republic of China

Received 28 August 2001; accepted 8 January 2002

ABSTRACT: The glass transition temperature of the hard-segment phase and the storage modulus of segmented polyurethane increased substantially in the presence of a small amount of tethered nano-sized layered silicates from montmorillonite compared with their pristine state (by 44°C and by 2.8-fold, respectively). Furthermore, the heat resistance and degradation kinetics of these montmorillonite/polyurethane nanocomposites were enhanced, as shown by thermogravimetric analysis. In particular, a 40°C increase in the degradation temperature and a 14% increase in the degradation activation energy occurred in polyurethane containing 1 wt % trihydroxyl swelling agent-modified montmorillonite compared to that of the pristine polyurethane. © 2002 Wiley Periodicals, Inc. J Appl Polym Sci 86: 1741–1748, 2002

Key words: polyurethanes, glass transition, mechanical properties, heat resistance, degradation

INTRODUCTION

Polyurethane, consisting of alternating soft and hard segments, displays a two-phase morphology. The hard-segment phase is derived from aggregation of urethane units through strong hydrogen bonding and is either glassy or semicrystalline. The soft-segment phase is composed of flexible chains such as polyether or polyester diol, and typically exhibits glass transition temperatures lower than room temperature. The functions of the two phases in polyurethane are different; the hard-segment phase is a major contributor to the modulus of polyurethane, and the flexible soft-segment phase predominantly influences the elastic nature of polyurethane.

The thermal properties of the segmented polyurethane depend largely on its overall composition, molecular weight, hydrogen bonding, and processing history. The glass transition temperature of the soft-segment phase of polyurethane has been studied extensively with differential scanning calorimetry (DSC) by several groups,[1–5] whereas the glass transition of the hard-segment phase of polyurethane cannot be detected by DSC measurements owing to its rather small heat capacity.[5] The determination of the glass transition temperature of the pure hard-segment phase has been attempted by extrapolating the glass transition temperatures of the phase-mixed polyurethanes of different hard-segment contents.[4,5] However, the actual glass transition temperature of the hard-segment phase still remains ambiguous by DSC. Hence, the more sensitive dynamic mechanical analysis (DMA) is applied to the determination of the glass transition of the hard-segment phase of polyurethane using the dissipation factor (tan δ), which is the ratio of the loss modulus to the storage modulus.[1,2, 6,7]

The onset of the thermal degradation of polyurethane usually initiates from the urethane bonds of the hard segments when the temperature is above 200°C, followed by an oxidation of the soft-segment phase.[8–10] For example, in the case of a polyurethane consisting of 4,4′-diphenylmethane diisocyanate (MDI), 1,4-butanediol (1, 4 BD) and polytetramethylene glycol (PTMEG), the decomposition of polyurethane is initiated from MDI-BD[9] following oxidation at the β-carbon next to the ether bond of soft segments (PTMEG), which then breaks the C—O bond and subsequently unzips the molecular chain through several stages.[10] The degradation of polyurethane is a rather complicated process as detected by several instruments such as thermo gravimetric analyses (TGA), Fourier Transform Infrared (FTIR), and mass spectrometer (MAS).[11–14]

Layered silicate/polymer nanocomposites have attracted a great deal of attention recently owing to the

Correspondence to: K. W. Wei (khwei@nctu.edu.tw).
Contract grant sponsor: National Science Council; contract grant number: NSC 90-2216-E-009-007.

improvements in the thermal, mechanical, and gas-barrier properties compared with those of the pristine polymers just by having a small amount of dispersed layered silicates. Several types of polymer nanocomposites such as polyamide,[15–17] epoxy,[18] polystyrene,[19] polyethylene oxide,[20] polyimide,[21–25] and polyurethane,[26–33] with layered silicates have been developed. One of the most abundant silicate sources is from natural montmorillonite. Natural montmorillonite is composed of disk-shaped silicates. The montmorillonite used in this study, trade name Swy-2, has flake shape, with many corners and a wide size distribution between 50 and 1000 nm. These silicate flakes contain ionic bonds in the intergallery and dangling hydroxyl groups on the surface of the silicates. In their pristine state, these silicates are highly hydrophilic and incompatible with organic polymers.[34] To improve the affinity of montmorillonite toward organic materials, it is necessary to modify montmorillonite by replacing the metal cations in the intergallery of the silicates with various organic cation molecules (swelling agents), whose size and reactivity affect the dispersion of the silicates in the polymer matrix.

The mechanical properties of polyurethane were found to improve substantially in the presence of silicates modified with nonreactive alkyl or aromatic organic molecules.[26–28,30–32] But, the enhancement of the thermal durability of polyurethane by silicates has rarely been demonstrated. In terms of thermal properties, the swelling agents often remain in their original chemical structures (low molecular weight) in the nanocomposites, and therefore produce a negative effect on the thermal resistance of the nanocomposites.

It has been reported that some of the swelling agents involved in the polymerization process can result in an exfoliated structure of silicates in the polymer and improved properties.[15–19,25,33] Therefore, we are motivated to improve the thermal properties of these nanocomposites by adopting an approach of modifying montmorillonite first with reactive swelling agents containing from one to three hydroxyl groups, and then treating the swelling agent as a pseudochain extender along with the regular chain extender, 1,4-butanediol, for a reaction with the isocyanate groups of polyurethane prepolymer to extend its chain length.[33] The detailed process is illustrated in the example of the trihydroxyl swelling agent-modified montmorillonite (3OH-Mont) case as shown in Figure 1. In Figure 1, the trihydroxyl swelling agent first forms ionic bonds with the silicates, and then its hydroxyl functional groups react with the isocyanate groups of the polyurethane prepolymer chains to establish urethane bonds in the first extension step. The regular chain extender, 1,4-butanediol, was added in the second extension step to complete the polymerization of polyurethane. Such a synthesis sequence resulted in a chemical structure in which the silicates are

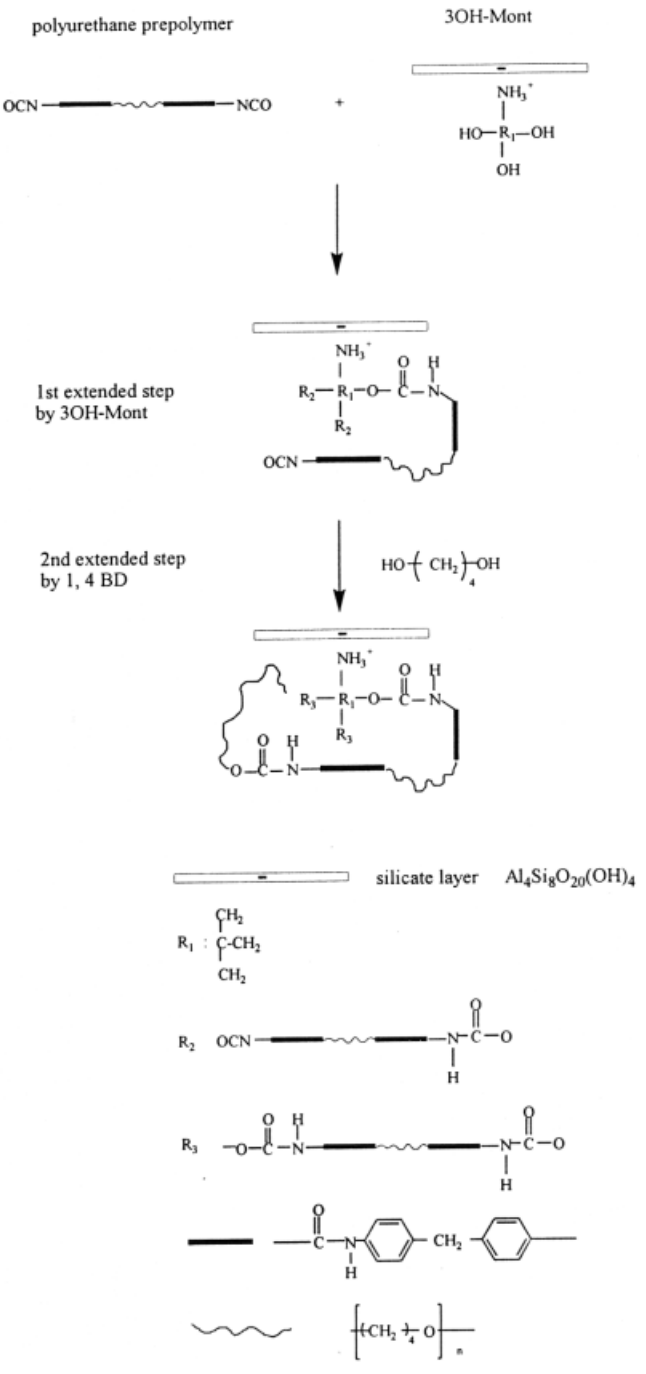

Figure 1 Schematic drawing of the molecular architecture of tethered layered silicates/polyurethane nanocomposites through reactive swelling agent containing trihydroxyl groups.

most likely tethered to the hard segments, which can protect the least stable urethane bonds in the polyurethane during heating. In this kind of nanostructured material, the existence of nano-sized silicates will quite possibly enhance the thermal properties of the polymer and hinder the mobility of the molecules in the hard-segment phase. The objectives of the present study are to understand the effects of silicates on the glass transition, dynamic mechanical properties, and

TABLE I
Compositions, Glass Transition Temperatures, and Storage Modulus of PU39 Nanocomposites Containing Different Amounts of Swelling Agent-Modified Montmorillonite

			DSC	DMA		
	MDI/PTMEG/1,4 BD/swelling agents[a]	Contents of SAM-Mont (wt%)	$Tg_{(soft)}$[b] (°C)	$Tg_{(soft)}$[c] (°C)	$Tg_{(hard)}$ (°C)	E'[d] $_{25\ °C}$ (MPa)
PU39	2/1/1/0	0	−53	−25	32	21
	2/1/0.997/0.003	1	−52	−26	41	33
1OH-Mont/PU39	2/1/0.991/0.009	3	−52	−24	43	37
	2/1/0.984/0.016	5	−53	−25	63	31
	2/1/0.994/0.006	1	−54	−26	45	41
2OH-Mont/PU39	2/1/0.982/0.018	3	−52	−25	47	44
	2/1/0.969/0.031	5	−53	−24	65	40
	2/1/0.991/0.009	1	−53	−26	60	76
3OH-Mont/PU39	2/1/0.972/0.028	3	−52	−24	71	79
	2/1/0.953/0.047	5	−53	−25	76	68

[a] Equivalent weight ratio (NCO/OH).
[b] Glass transition temperature of soft-segment phase obtained from DSC.
[c] Glass transition temperature of soft-segment phase obtained from DMA.
[d] Storage modulus at 25°C.

thermal degradation kinetics of polyurethane through DSC, DMA, and TGA analyses.

EXPERIMENTAL

Materials

Swy-2 montmorillonite, having a cationic exchange capacity of 76.4 mEq/100 g, was obtained from the Clay Minerals Depository at the University of Missouri, Columbia, MO. Swelling agents such as 3-amino 1-propanol (99%, Acros), 3-amino 1, 2-propanediol (98%, Acros) and trishydroxymethyl aminomethane (99%, Merck), were used as received, and they were termed as 1OH, 2OH, and 3OH, respectively. The detailed process of preparing swelling agent-modified montmorillonites (SAM-Monts) has been described elsewhere.[23] Montmorillonite modified with 1OH, 2OH, and 3OH was noted as 1OH-Mont, 2OH-Mont, and 3OH-Mont, respectively. The amount of swelling agent in these SAM-Monts can be calculated from the exchanged portion of sodium cations in the intergalleries, as determined by the difference in the weight loss percentages of the pristine montmorillonite and of the SAM-Mont in the temperature range between 120 and 800°C.[17] The TGA results show that the portion of sodium cations exchanged by the swelling agent was about 50%. Polytetramethylene glycol (PTMEG, M_n = 1000, Aldrich) was dehydrated under vacuum in an oven at 60°C for 2 days. 4,4′-diphenylmethane diisocyanate (MDI, Aldrich) was melted and pressure filtered under N_2 at 60°C followed by recrystallization from hexane in an ice bath. Dimethylformamide (DMF, 99%, Fisher) and 1,4-butanediol (1,4 BD, Lancaster) were dried over calcium hydride for 2 days and then were vacuum distilled. Polyurethane containing 39 wt % hard segment (PU39) was produced by first reacting MDI and PTMEG at an equivalent weight ratio of 2 : 1 in 35 mL DMF solvent at 90°C for 2 h to form the prepolymer. Then, 1,4 BD in 10 mL DMF was added to the prepolymer solution and was stirred for another 2 h to form polyurethane solution whose solid content was 30% by weight. Subsequently, the solution was cast in a mold to heat at 70°C for 24 h to complete the polymerization and remove the solvent. For preparing the swelling agent-modified montmorillonites (SAM-Monts)/polyurethane nanocomposites, the prepolymer was synthesized by the same procedure as that of the pure polyurethane, and then different amounts of SAM-Monts were added with stirring for 2 h and followed by adding 1,4 BD with stirring for another 2 h. The nanocomposite solution was heated at 70°C for 24 h in a mold to complete the polymerization. The contents of SAM-Monts in these nanocomposites were 1, 3, and 5 wt %. The ratio of isocyanate (NCO) to hydroxyl (OH) was kept at 1 for all polyurethane nanocomposites, and the detailed compositions of these samples are given in Table I.

Characterization

Wide-angle X-ray diffraction (WAXD) experiments were performed by using a Mac Science M18 X-ray diffractometer. The X-ray beam was generated from nickel-filtered Cu Kα (λ = 0.154 nm) radiation in a sealed tube operated at 50 kV and 250 mA. The diffraction curves were obtained from 3 to 10° at a scan rate of 1°/min. Samples for transmission electron microscopy study were first microtomed with a Leica Ultracut Uct into about 90-nanometer-thick slices at −80°C, and then they were observed with a transmission electron microscope (TEM) of model JOEL-2000FX.[31] Differential scanning calorimetry analyses,

over the temperature range from −100 to 220°C, were conducted with a Dupont DSC 2910 at a heating rate of 20°C/min under a nitrogen purge. Dynamic mechanical analyses were carried out by using a Dupont DMA 2980 with a dual cantilever head on films with dimensions of 40 × 8 × 0.5 mm at a frequency of 1 Hz and heating rate of 3°C/min from −100 to 200°C. The degradation kinetics study of polyurethane nanocomposites was carried out by using a Dupont TGA 2950. Samples about 10 mg for thermogravimetric kinetic analysis were heated from 25 to 800°C at heating rates of 1, 5, 10, and 20°C/min, respectively, under a steady nitrogen atmosphere (50 mL/min) after the water was removed in an oven at 60°C for 48 h.

RESULTS AND DISCUSSION

The wide-angle X-ray diffraction (WAXD) curves of montmorillonite (Mont) and swelling agent-modified montmorillonites (SAM-Monts) are shown in Figure 2(a). In Figure 2(a), the appearance of a broad diffraction peak at $2\theta = 7.4°$ for the pure montmorillonite indicated that the intergallery d-spacing between the rather isotropic silicates was about 1.2 nm. The diffraction peak at $2\theta = 5.8°$ appeared in each of the WAXD curves of 1OH-Mont, 2OH-Mont, and 3OH-Mont, and only one of them, which is noted as SAM-Monts, is demonstrated in Figure 2(a). Hence, the d-spacing of SAM-Monts has been increased to 1.5 nm, and the resemblance in the d-spacings of these SAM-Monts can be ascribed to the fact that the molecular lengths of the three swelling agents, 1OH, 2OH, and 3OH, are about the same. There were two medium diffraction peaks at $2\theta = 5.0°$ and at $2\theta = 5.2°$, yielding d-spacings of 1.8 and 1.7 nm, for PU39 containing 3 and 5 wt % 1OH-Mont cases, respectively. In the 2OH-Mont/PU39 case, one diffraction peak at $2\theta = 5.0°$, corresponding to a d-spacing of 1.8 nm, occurred for the 5 wt % 2OH-Mont composition. No WAXD peak appeared for the 3OH-Mont/PU39 system, implying that the layered silicates have been either intercalated to a distance of more than 3 nm d-spacing or exfoliated in the polyurethane. The superstructure of these polyurethane nanocomposites resembling the hierarchical structure in Akelah's article[35] displayed an intercalated morphology of layered silicates from the transmission electron microscopy study. The domain sizes of the intercalated silicates ranged from 100 to 500 nm. A typical morphology of the dispersion of silicates in the polyurethane is presented in the TEM micrograph of PU39 containing 3 wt % 3OH-Mont as shown in Figure 2(b). In Figure 2(b), the space between the layered silicates is about 4 to 7 nm, and a portion of silicates displayed exfoliated structures.

The DSC results of these nanostructured polyurethanes are given in Table I. In Table I, the glass transition temperature of the soft-segment phase ($T_{g,\text{soft}}$) of

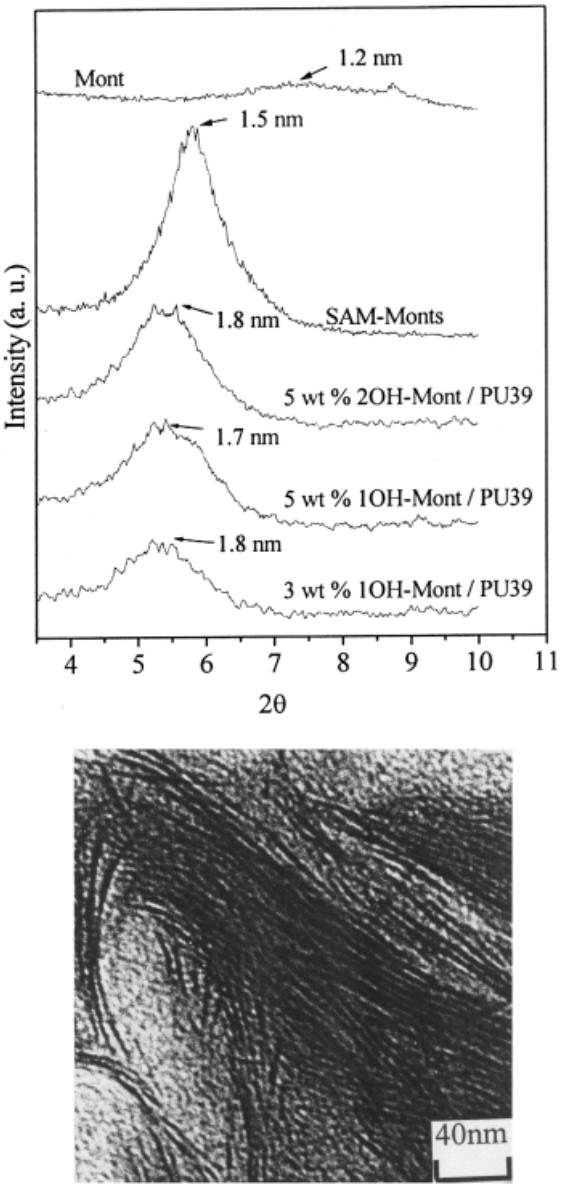

Figure 2 (a) The wide-angle X-ray diffraction curves of montmorillonite (Mont), swelling agent-modified montmorillonites (SAM-Monts), and PU39 containing different amounts of SAM-Monts (b) transmission electron microscopy micrograph of the cross section view of PU39 nanocomposite containing 3 wt % 3OH-Mont.

PU39 was −53°C, and there was essentially no change in the glass transition temperatures of the soft-segment phase of the PU39 nanocomposites of various compositions because DSC cannot probe the glass transition temperature of polymer chains close to the silicates. Thus, the measured glass transition temperature is that of the soft-segment phase far away from the silicates, and is the same as that of the bulk polyurethane. The glass transition of the hard-segment phase of the pristine polyurethane was not detectable in the DSC measurements because of low hard-segment content and a rather small heat capacity difference at its glass transition ($\Delta C_{p(\text{hard})} = 0.38$ J/g °C).[5]

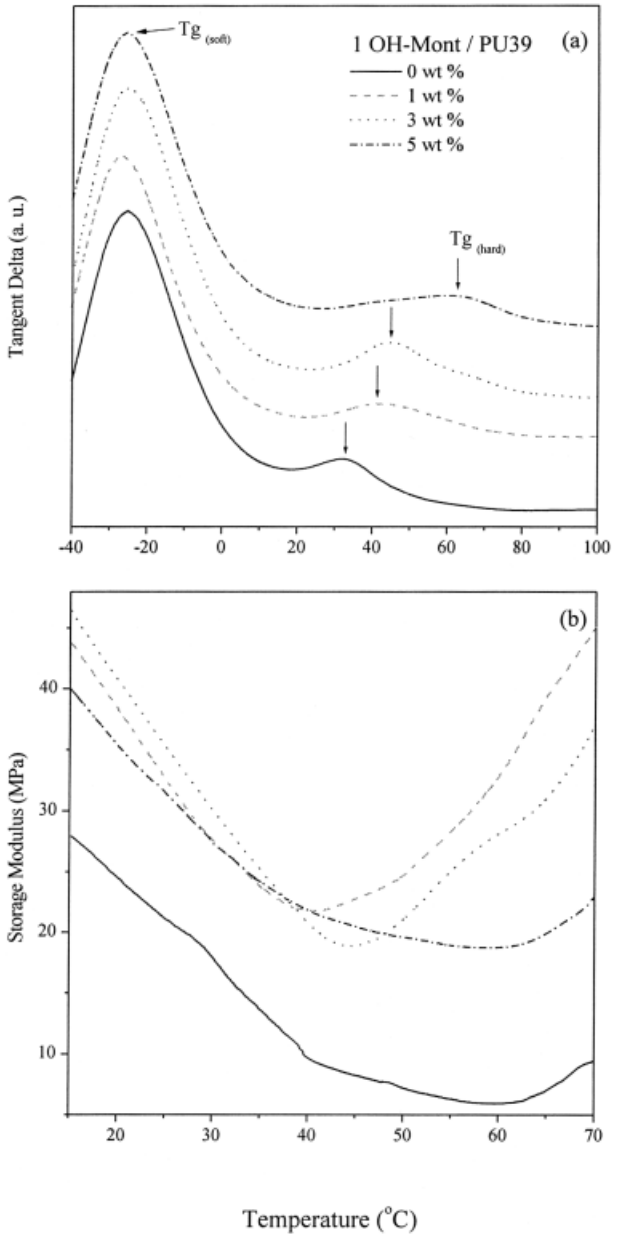

Figure 3 (a) The dissipation factor (tan δ) and (b) the storage modulus (E') of PU39 nanocomposites containing different amounts of 1OH-Mont at different temperatures.

The dynamic mechanical analysis results for the determination of the glass transition of the hard-segment phase of the polyurethane are demonstrated in Figures 3 and 4. The complete peak positions in the tan δ curves and storage modulus at 25°C are summarized in Table I. In Figure 3(a), one large peak at −25°C and one small peak at 32°C were displayed in the tan δ curve of pure PU39. The large low-temperature tan δ peak is attributed to the backbone motion in the soft-segment phase of the PU39 molecules and is defined as $T_{g,soft}$,[1,2,6] whereas the small tan δ peak at high temperature is due to the molecular motion of the amorphous region in the semicrystalline hard-segment phase and is noted as $T_{g,hard}$.[7] The glass transition temperatures of the soft-segment phase of PU39 nanocomposites showed no change compared with that of the pristine PU39 by DMA, and were higher than those obtained from the DSC measurements. This dependency of T_g on the analyzing methods has been well described elsewhere.[36] Notably, the glass transition temperatures of the hard-segment phase of PU39 nanocomposites increased with the amount of swelling agent-modified montmorillonite. For the case of 1OH-Mont/PU39 in particular, the glass transition temperatures of the hard-segment phase of PU39 containing 1, 3, and 5 wt % 1OH-Mont were 9, 11, and 13°C higher than that of pristine PU39, respectively,

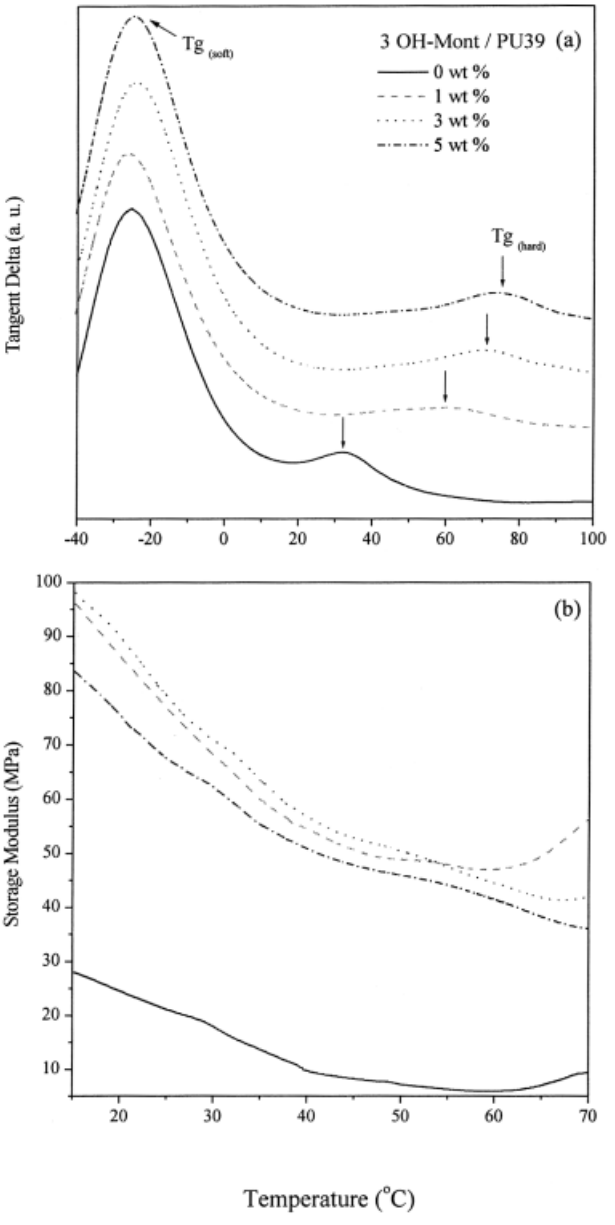

Figure 4 (a) The dissipation factor (tan δ) and (b) the storage modulus (E') of PU39 nanocomposites containing different amounts of 3OH-Mont at different temperatures.

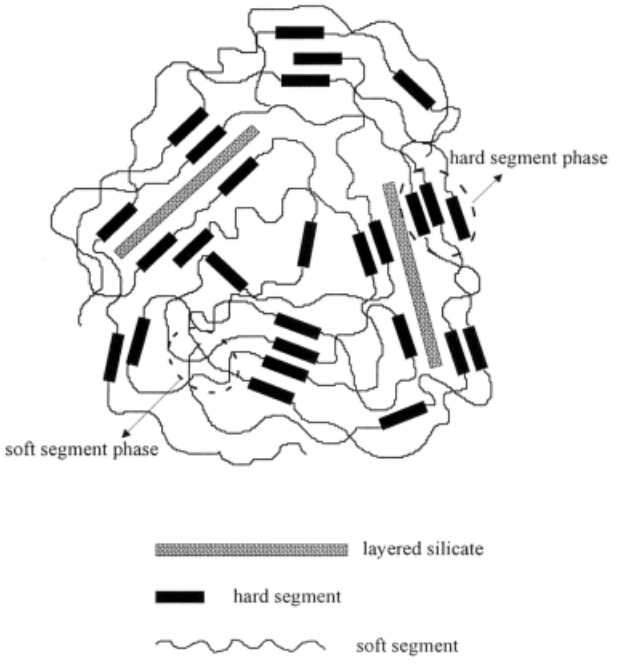

Figure 5 The schematic drawing of reactive swelling-agent-modified silicate dispersing in polyurethane.

implying that the nano-sized silicates hindered the movement of molecules in the hard-segment phase. The extent of increase in the glass transition temperature of the hard-segment phase of PU39 nanocomposites due to the presence of silicate layers also depends on the number of hydroxyl groups in the swelling agent. The largest increase, 44°C, in the glass transition temperature of the hard-segment phase, compared to that of the pure PU39, occurred in the case of PU39 containing 5 wt % 3OH-Mont. This behavior is due to the increase in the exfoliation of silicates in PU39 because the interfacial area between silicates and polyurethane increased with the extent of exfoliation. The larger the interfacial area between the silicates and the polyurethane, the stronger the hindrance of the movement of the hard segments. The schematic of the speculated molecular architecture of the nanocomposites is shown in Figure 5. In Figure 5, layered silicates are mostly surrounded by the hard segments except for a small portion of the silicates. The chemical reason for this nanostructure is that the hydroxyl groups of the swelling agents attaching to the silicates tend to react readily with the isocyanate groups of the prepolymer during the synthesis, resulting in a tethering of the silicates onto the polyurethane molecules. Additionally, the urethane bonds in the hard segments can form hydrogen bonding with the dangling hydroxyl groups on the surface of the silicates. Table I shows that the storage modulus (E') of PU39 nanocomposites increased dramatically compared with that of pristine PU39. At 25°C, 76%, 1.1-fold and 2.8-fold increases in the storage modulus were found for PU39 nanocomposites containing 3 wt % 1OH-Mont, 2OH-Mont, and 3OH-Mont, respectively, compared with that of pristine PU39, due to the reinforcement of the hard-segment phase of PU39 by the tethered nano-sized silicates. However, the storage modulus of these PU39 nanocomposites decreased when the amount of SAM-Mont was more than 3 wt %. This behavior can be attributed to the fact that the molecular weight and the hydrogen bonding in the hard-segment phase of the polyurethane decrease with the increasing amount of layered silicates.[31]

The degradation of polyurethane involves two stages: the first stage is dominated by the degradation of the hard segment, and the second stage correlates well with the dissociation of the soft segment.[10] In Figure 6(a) and (b), the temperature at 5% weight loss, the peak temperatures of the first degraded stage and the second stage are defined as T_d, $T_{1\max}$ and $T_{2\max,}$ respectively. The complete results of these thermal characteristics of pristine PU39 and PU39 nanocomposites measured at 1°C/min and 20°C/min heating rates are given in Table II. These temperatures of PU39 nanocomposites were all higher than those of pristine polyurethane, indicating the nano-sized silicates can enhance the heat resistance of polyurethane. As reported in previous studies,[8,10,37] the inception of thermal degradation of the pristine PU39 started at around 308°C. In Table II, the degradation temperatures of PU39 containing 1 wt % 1OH-Mont, 2OH-Mont, and 3OH-Mont measured at a 20°C/min heating rate were 17, 30, and 40°C higher than that of pristine PU39, respectively. Because the presence of layered silicates enhances the thermal stability of PU39, it provides another piece of indirect evidence that a large portion of layered silicates is distributed in the hard-segment phase. As for other thermal characteristics such as $T_{1\max}$ and $T_{2\max}$ of PU39 nanocomposites, the data suggest the same trend in thermal enhancement. The characteristics of the degradation of PU39 nanocomposites changed with the heating rate due to the variation in heat diffusion. In Table II, the heat resistance of PU39 nanocomposites increased with the number of hydroxyl groups of the swelling agents, resulting from a more exfoliated silicate in polyurethane. In addition, the extent of enhancement in the thermal stability of PU39 nanocomposites by silicates reached its maximum value when the content of SAM-Mont was at 1 wt %. This can be attributed to the extent of reduction in the molecular weight of polyurethane with the increased SAM-Mont content.[33]

The activation energy of degradation at different conversions during heating can be obtained by kinetics analyses using the Ozawa, Flynn, and Salin models.[11–14] In the present study, the TGA degradation kinetics data of pristine PU39 and PU39 nanocomposites were fitted with the Ozawa model.[10–11,13,14] The data are plotted by the logarithm of heating rate

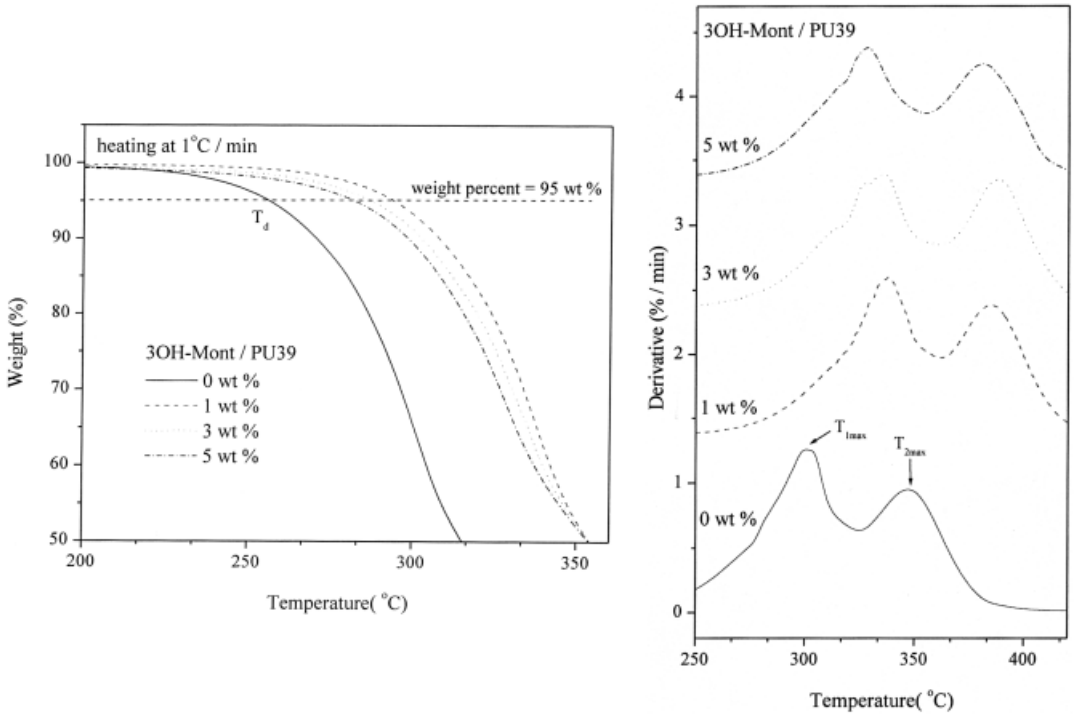

Figure 6 (a)TGA and (b) DTGA curves of PU39 containing different amounts of 3OH-Mont measured at 1°C/min heating rate.

($\log_{10}\beta$) against the reciprocal absolute temperature ($1/T$) for each conversion degree (α), defined as the weight loss at a given temperature. The suitable range of conversion degree for the Ozawa model is smaller than 0.9.[38] From the isoconversion curves, activation energy (E_a) at the specific conversion can be obtained from the equation:

$$Ea = \frac{-\text{ slope} \times R}{0.457}$$

where R is the gas constant, and the calculated results of PU39 and PU39 nanocomposites between 0.05 to 0.4 conversions are given in Table II.

The activation energies in the degradation of PU39 increased from 140 kJ/mol at 10% conversion to 147 kJ/mol at 30% conversion but decreased to 138 kJ/mol at 40% conversion. This behavior is consistent with the results of other articles.[10,12] The activation energies of degradation of PU39 nanocomposites were higher than those of PU39 because the tethered silicates

TABLE II
Thermal Characteristics and Activation Energy of Degradation at Different Conversions of Pristine PU39 and PU39 Nanocomposites

		Heat at 1 °C/min			Heat at 20 °C/min			Activation energy (Ea, kJ/mole)				
	Contents of Mont (wt %)	T_d[a] (°C)	T_{1max}[b] (°C)	T_{2max}[c] (°C)	T_d[a] (°C)	T_{1max}[b] (°C)	T_{2max}[c] (°C)	α^d =0.05	α^d = 0.1	α^d = 0.2	α^d = 0.3	α^d = 0.4
PU39	0	256.2	303.8	349.1	308.1	344.7	421.3	140	140	146	147	138
	1	273.1	314.8	370.3	325.4	363.0	439.6	149	144	152	156	157
1OH-Mont/PU39	3	267.5	311.0	369.8	321.2	362.7	439.3	142	142	147	153	154
	5	262.1	306.0	369.1	316.8	363.2	439.8	139	141	143	146	145
	1	283.4	325.0	383.3	338.5	375.4	452.1	148	149	156	159	159
2OH-Mont/PU39	3	278.5	322.6	374.3	332.3	373.0	446.2	147	145	151	154	145
	5	271.9	317.7	380.6	325.7	370.8	447.4	143	144	143	149	145
	1	294.8	338.1	386.4	348.1	384.1	460.7	159	157	167	168	158
3OH-Mont/PU39	3	287.7	335.5	388.4	339.1	381.8	458.3	157	155	159	161	154
	5	282.1	327.1	381.1	337.3	382.4	455.7	147	147	149	152	146

[a] Temperature at 5% weight loss obtained form TGA curve.
[b] The peak temperature of the first degraded stage obtained from DTGA curve.
[c] The peak temperature of the second degraded stage obtained from DTGA curve.
[d] The weight loss at a given temperature.

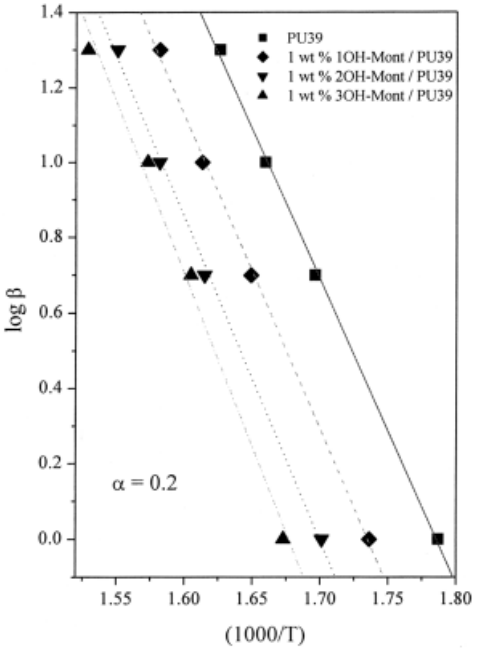

Figure 7 The dependence of $\log_{10}\beta$ on $1/T$ for PU39 containing 1 wt % swelling agent-modified montmorillonite at 20% conversion.

served as a thermal barrier for delaying the hard segments from degradation during heating. Nevertheless, the thermal stability of PU39 nanocomposites decreased as the amount of silicate in PU39 was increased to more than 1 wt %. For example, in the case of PU39 containing different amounts of 1OH-Mont at 10% conversion, the maximal activation energy, 4 kJ/mol higher than that of pristine PU39, occurred in PU39 containing 1 wt % 1OH-Mont, attributed to a better dispersion of the silicates in the polyurethane at low silicate content. Additionally, the plot of $\log_{10}\beta$ vs. $1000/T$ of PU39 containing 1 wt % SAM-Mont is shown in Figure 7. At 20% conversion, the activation energies of PU39 containing 1 wt % 1OH-Mont, 2OH-Mont, and 3OH-Mont were 4, 7, and 14% higher than that of pristine PU39, respectively. The largest increase in activation energy occurred in PU39 containing 1 wt % 3OH-Mont, which resulted from its exfoliated silicate structure and the compensated effect of the trihydroxyl swelling agent on the reduced molecular weight of the polyurethane.

CONCLUSIONS

The introduction of a small amount of tethered nanosized layered silicates into segmented polyurethane leads to a substantial increase in its hard-segment phase's glass transition temperature and storage modulus. Moreover, the thermal stability of the polyurethane was also greatly enhanced by the presence of the exfoliated silicates. Specifically, a 40°C increase in degradation temperature and a 14% increase in the activation energy at 20% conversion occurred in PU39 containing 1 wt % trihydroxyl swelling agent-modified silicate compared with that of pristine PU39.

We appreciate the financial support provided by National Science Council through project NSC 90-2216-E-009-007.

References

1. Miller, J. A.; Lin, S. B.; Hwang, K. S.; Wu, K. S.; Gibson, P. E.; Copper, S. L. Macromolecules 1985, 18, 32.
2. Wang, C. B.; Cooper, S. L. Macromolecules 1983, 16, 775.
3. Koberstein, J. T.; Calambos, A. F.; Leung, L. M. Macromolecules 1992, 25, 6195.
4. Leung, L. M.; Koberstein, J. T. Macromolecules 1986, 19, 706.
5. Chen, T. K.; Chui, J. Y.; Shieh, T. S. Macromolecules 1997, 30, 5068.
6. Ryan, A. J.; Stanford, J. L.; Still, R. H. Polymer 1991, 32, 1426.
7. Ng, H. N.; Allegrezza, A. E.; Seymour, R. W.; Cooper, S. L. Polymer 1973, 14, 255.
8. Shieh, Y. T.; Chen, H. T.; Liu, K. H.; Two, Y. K. J Polym. Sci A Polym Chem 1999, 37, 4126.
9. Yang, W. P.; Macosko, C. W.; Wellinghoff, S. T. Polymer.1986, 27, 1235.
10. Petrovic, Z. S.; Zavargo, Z.; Flynn, J. H.; Macknight, W. J. J Appl Polym Sci. 1994, 51, 1087.
11. Chang, C. T.; Shen, W. S.; Chiu, Y. S.; HO, Y. S. Polym Degrad Stabil 1995, 49, 353.
12. Lage, L. G.; Kawano, Y. J Appl Polym Sci. 2001, 79, 910.
13. Suhara, F.; Kutty, S. K. N.; Nando, G. B. Polym Degrad Stabil 1998, 61, 9.
14. Lin, M. F.; Tsen, W. C.; Shu, Y. C.; Chuang, F. S. J Appl Polym Sci 2001, 79, 881.
15. Usuki, A.; Kawasumi, M.; Kojima, Y.; Okada, A.; Kurauchi, T.; Kamigaito, O. J Mater Res 1993, 8, 1174.
16. Usuki, A.; Kawasumi, M.; Kojima, Y.; Okada, A.; Fukushima, Y.; Kurauchi, T.; Kamigaito, O. J Mater Res 1993, 8, 1179.
17. Kojima, Y.; Usuki, A.; Kawasumi, M.; Okada, A.; Kurauchi, T.; Kamigaito, O. J Polym Sci A Polym Chem 1993, 31, 983.
18. Wang, Z.; Pinnavaia, T. J Chem Mater 1998, 10, 1820.
19. Weimer, M. W.; Chen, H.; Giannelis, E. P.; Sogah, D. Y. J Am Chem Soc 1999, 121, 1615.
20. Hackett, E.; Manias, E.; Giannelis, E. P. Chem Mater 2000, 12, 2161.
21. Lan, T.; Kaviratna, P. D.; Pinnavaia, T. J Chem Mater 1994, 6, 573.
22. Tyan, H. L.; Liu, Y. C.; Wei, K. H. Polymer 1999, 40, 4877.
23. Tyan, H. L.; Liu, Y. C.; Wei, K. H. Chem Mater 1999, 11, 1942.
24. Tyan, H. L.; Wei, K. H.; Hsieh, T. E. J Polym Sci Polym Phys 2000, 38, 2873.
25. Tyan, H. L.; Leu, C. M.; Wei, K. H. Chem Mater 2001, 13, 222.
26. Wang, Z.; Pinnavaia, T. J Chem Mater 1998, 10, 3769.
27. Zilg, C.; Thomann, R.; Mulhaupt, R.; Finter, J. Adv Mater 1999, 11, 49.
28. Xu, R.; Manias, E.; Snyder, A. J.; Runt, J. Macromolecules 2001, 34, 337.
29. Chen, T. K.; Tien, Y. I.; Wei, K. H. J Polym Sci Polym Chem 1999, 37, 2225.
30. Chen, T. K.; Tien,Y. I.; Wei, K. H. Polymer 2000, 41, 1345.
31. Tien, Y. I.; Wei, K. H. Polymer 2001, 42, 3213.
32. Tien, Y. I.; Wei, K. H. J Polym Res. 2000, 7, 245.
33. Tien, Y. I.; Wei, K. H. Macromolecules. 2001, 34, 9045.
34. Pinnavaia,T. J. Science 1983, 220, 365.
35. Akelah, A.; Salahuddin, N.; Hiltner, A.; Baer, E.; Moet, A. Nanostruct Mater 1994, 4, 965.
36. Sperling, H. L. In Introduction to Physical Polymer Science; John Wiley: New York, 1992, p. 317, 2nd ed.
37. Hu, W. C.; Koberstein, J. T. J Polym Sci Polym Phys 1994, 32, 437.
38. Ozawa, T. Bull Chem Soc Jpn 1965, 38, 1881.